Charged Particles on Surfaces: Coexistence of Dilute Phases and Periodic Structures at Interfaces

Sharon M. Loverde,[1] Francisco J. Solis,[2] and Monica Olvera de la Cruz[1]

[1]*Department of Materials Science and Engineering, Northwestern University, Evanston, Illinois 60208-3108, USA*

[2]*Integrated Natural Sciences, Arizona State University West, Phoenix, Arizona 85069, USA*

(Received 6 November 2006; published 6 June 2007)

We consider a mixture of two immiscible oppositely charged molecules strongly adsorbed to an interface, with a neutral nonselective molecular background. We determine the coexistence between a high density ionic periodic phase and a dilute isotropic ionic phase. We use a strong segregation approach for the periodic phase and determine the one-loop free energy for the dilute phase. Lamellar and hexagonal patterns are calculated for different charge stoichiometries of the mixture. Molecular dynamics simulations exhibit the predicted phase behavior. The periodic length scale of the solid phase is found to scale as $\varepsilon/(l_B\psi^{3/2})$, where ψ is the effective charge density, l_B is the Bjerrum length, and ε is the cohesive energy.

DOI: 10.1103/PhysRevLett.98.237802 PACS numbers: 61.20.Gy, 68.47.Pe

Phase separation phenomena and pattern formation at surfaces [1,2] are areas of great scientific interest. Recent studies have shown that mixtures of immiscible oppositely charged molecules can form periodic nanostructures [3–5]. The competition of short range and long range interactions leads to the formation of periodic structures in a multitude of systems, including lipid Langmuir monolayer mixtures [6–8], two-dimensional (2D) uniaxial ferromagnets [9], reaction controlled phase segregating mixtures [10], two-dimensional electron gases in metal-oxide-semiconductor field-effect transistors [11], and responsive gels [12]. We explore here the case of patterns formed by charged molecules adsorbed onto biological membranes and other neutral surfaces, including liquid interfaces such as emulsions when cationic and anionic macromolecules are adsorbed onto the interface. Oppositely charged components adsorbed onto interfaces may form ionic domains reminiscent of biological rafts. The competition between electrostatics and immiscibility may give rise to a periodic solid phase that coexists with a dilute charged gas at the interface. In this Letter, we determine the boundary of the coexistence region between the dilute gas and the periodic solid phase for varying degrees of chemical incompatibility and stoichiometric ratios of the adsorbed molecules.

We use analytic techniques and molecular dynamics simulations of a coarse-grained model as shown in Fig. 1(a). In the model, we do not wish to study the adsorption or desorption to the interface but the phase behavior assuming a constant interfacial area. We assume that the monolayer surface is in equilibrium and that fluctuations perpendicular to the interface are negligible. First, we explore the phase behavior of this model analytically when the ionic domains are well-segregated periodic nanostructures and the dilute phase is treated as a gas of charges. We then describe the results of molecular dynamics simulations for intermediate segregation regimes.

We consider the coexistence of two possible phases at low temperature. One phase consists of a dense, patterned solid formed by the oppositely charged components. Its free energy is computed by assuming the formation of regions of constant particle and charge density. The second phase is homogenous and has a low density of charged particles. It is treated as a two-dimensional charged gas in a homogenous background that displays nonselective interactions with the charged components. The free energy of the low density homogenous gas of charged particles is calculated using linear response theory by means of the one-loop approximation or random phase approximation (RPA) [13] at the interface. The phase diagram is plotted in Fig. 1.

The periodicity of the domains in the solid phase is lamellar for nearly symmetric stoichiometric ratios, while, for asymmetric ratios, nearly circular domains are arranged in a hexagonal lattice. The average absolute value of the charge density is $\psi = f_+\psi_+ + f_-|\psi_-|$, where $f_\pm$ represents the area fraction of the components and $\psi_\pm$ their charge density. The free energy, per area A with periodicity L, has the form

$$\frac{F}{Ak_BT} = \gamma\frac{s_1}{L} + l_B\psi^2 s_2 L. \tag{1}$$

The Bjerrum length is $l_B = e^2/4\pi\epsilon k_BT$, k_B is the Boltzmann constant, T is the temperature, ϵ is the dielectric permittivity of the medium, and γ is the line tension between domains. The coefficients s_1 and s_2 are dimensionless quantities that depend on the specific shape of the domains, as explicitly defined in Ref. [3]. s_1 is the ratio of the interface length within a unit cell to the size of the cell. s_2 is the integral of the dimensionless Coulombic potential over the whole space, averaged over a unit cell. Minimizing the free energy with respect to the size L, we obtain a characteristic length $L_{\min} = (s_1/s_2)^{1/2}L_0$, with $L_0 = [\gamma/(l_B\psi^2)]^{1/2}$, and the free energy density is $2(s_1s_2)^{1/2}f_0/L_0^2$, where $f_0 = (\gamma l_B\psi^2)^{1/2}$ [3,14]. The net free energy of the solid phase also includes the cohesive

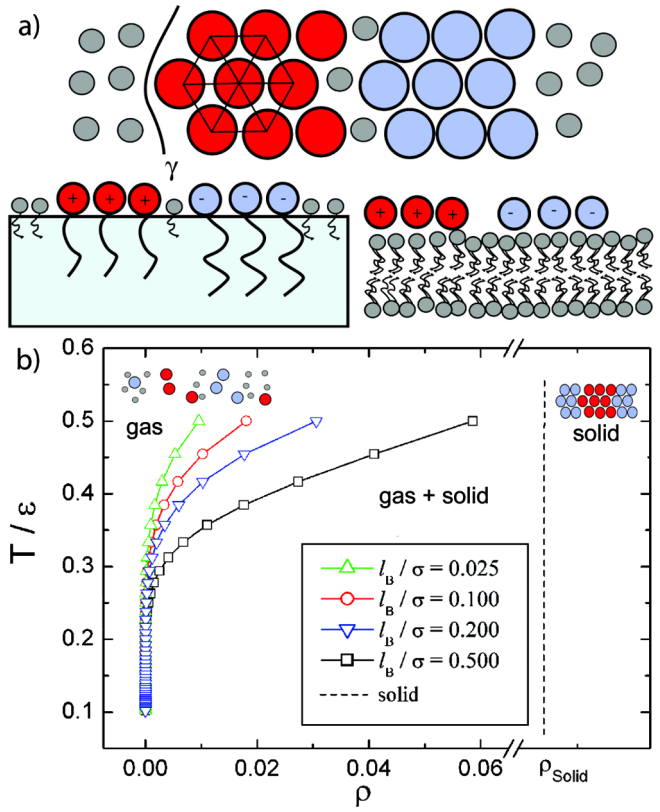

FIG. 1 (color online). (a) Schematic of neutral and charged components strongly adsorbed to an interface, such as an emulsion or the surface of a bilayer. The charged components segregate into a periodic solid phase with line tension γ between domains, with a homogenous background. (b) Phase diagram of the mixture. Location of solid-gas coexistence boundaries in the $\rho - T$ plane are shown for several different values of the Bjerrum length l_B/σ. Increasing l_B/σ requires higher values of short range interactions ε/T for phase coexistence. The figure refers to the case of equal charge density $z_+/z_- = 1$, which forms a lamellar microphase, with constant density ρ_{solid}.

energy that arises from segregation of the charged molecules from the neutral background. In our description of the solid phase, at low temperatures, we assume a constant density given by the hexagonal close packing (hcp) of spherical molecules of radius σ, corresponding to a density $\rho_{\text{solid}} = 1/\sqrt{3}\sigma^2$. The effective cohesive energy per unit area can be written in terms of ε, which corresponds to the net interaction between components, with 6 contacts between neighbors. The line tension is $\frac{\sqrt{6}\varepsilon}{\sigma}$. Inclusion of the cohesive energy leads the final result for the solid phase:

$$\frac{F_s(\rho_{\text{solid}})}{A} = -3\varepsilon\rho_{\text{solid}} + 2(s_1 s_2)^{1/2} f_0/L_0^2. \qquad (2)$$

The free energy of the gas phase is obtained from the partition function [13,15]

$$Z = Z_o \frac{V^N}{N!} \int \exp\Big(-\sum_{k\neq 0}\sum_{ij} \frac{\mathbf{A}_k^{ij}\rho_k^i \rho_{-k}^j}{2V}\Big) \prod_{k>0}\prod_i \frac{d\rho_k^i}{\pi V \rho_i},$$

where $\mathbf{A}_k^{ij} = \mathbf{U}_k^{ij} + \rho_i^{-1}\delta_{ij}$. Here ρ_i represents the density of the ith component, ρ_k represents the Fourier transform of the component densities, and k is the wave vector. Z_o includes the $k = 0$ and self-energy terms. $\mathbf{U}_k^{ij}$ is the sum of the interaction energies, consisting of the short range interactions due to the excluded volume and hydrophobic interaction as well as the long range contributions due to the electrostatic energy. The electrostatic contribution to the internal energy matrix uses the 2D Fourier transform of the screened Coulomb interaction $E_{\text{el}}^{ij} = 2\pi z_i z_j l_B (k^2 + \kappa^2)^{-1/2}$, where κ is the inverse screening length. The free energy is then

$$F = \sum_{ij} \frac{N_i(N_j - \delta_{ij})}{2V} U_o^{ij} + \sum_i N_i \ln\frac{\rho_i}{e} + \sum_{k>o}\Big[\ln\frac{\det|U_k^{ij} + \rho_i^{-1}\delta_{ij}|}{\det|\rho_i^{-1}\delta_{ij}|} - \sum_i \rho_i U_k^{ii}\Big], \qquad (3)$$

where U_0^{ij} includes the short range excluded volume of the components. The electrostatic contribution vanishes due to charge neutrality. The second term is the entropic term. The third term is the electrostatic contribution due to density fluctuations, calculated by integrating over possible values of k from 0 to $2\pi/a$, where a is the molecular size. The presence of salt does not change the periodicity significantly up to when the screening length is of the order of the domain size when the periodic phase decomposes into two macroscopically segregated phases of charges [3]. The electrostatic contribution, considering the limit of no screening due to ions in the surrounding solution ($\kappa \to 0$), is

$$\frac{F_{\text{el}}}{k_B T} = \frac{1}{4\pi}\Big[\frac{2\pi^2 \ln(1 + \frac{a k_{\text{in}}^2}{2\pi})}{a^2} + \frac{\pi k_{\text{in}}^2}{a} - \frac{1}{2}k_{\text{in}}^4 \ln\Big(1 + \frac{2\pi}{a k_{\text{in}}^2}\Big)\Big], \qquad (4)$$

where $k_{\text{in}}^2 = 2\pi l_B(\rho_+ z_+^2 + \rho_+ z_+^2)$, the internal screening due to ions in the plane. Upon considering the charge neutrality constraint $z_+\rho_+ = z_-\rho_-$, the total free energy per unit area of the gas phase, in terms of ρ ($\rho = \rho_+ + \rho_-$), is then

$$\frac{F_{\text{gas}}}{A k_B T} = \frac{\rho}{\alpha}\ln\Big(\frac{\rho}{\alpha e}\Big) + \frac{\rho}{\beta}\ln\Big(\frac{\rho}{\beta e}\Big) + \frac{\upsilon_{11}}{2}\Big(\frac{\rho}{\alpha}\Big)^2 + \frac{\upsilon_{22}}{2}\Big(\frac{\rho}{\beta}\Big)^2 + \upsilon_{12}\frac{\rho^2}{\alpha\beta} + \frac{F_{\text{el}}}{k_B T}, \qquad (5)$$

where $\alpha = 1 - (z_+/z_-)$ and $\beta = 1 - (z_-/z_+)$. The virial terms are $\upsilon_{ij} = -\int e^{-U_{ij}/k_B T} - 1$, where U_{ij} is a hard core potential from $0 < r < \sigma$ and a classic 6–12 Lennard-Jones potential from $\sigma < r < 2.5\sigma$.

The phase coexistence of the periodic solid and the dilute gas is obtained using the common tangent rule. Assuming a fixed solid density, the coexistence equation is

$$F_S\left(\frac{\rho_{\text{solid}}}{A}\right) = \frac{F_{\text{gas}}}{A} + (\rho_{\text{solid}} - \rho)\frac{\partial F_{\text{gas}}}{\partial \rho}. \quad (6)$$

The boundary of the coexistence region for low values of the gas phase density is shown in Fig. 1(b) for equal stoichiometric ratios $z_+/z_- = 1$. The coexistence lines depend on the relative strengths of the Coulomb interaction l_B/σ and on the cohesive or immiscibility parameter ε. With increasing l_B/σ, phase coexistence occurs at lower temperatures. We do not calculate for higher densities, when nonlinear corrections including short range correlations and ion association are necessary, to correctly describe the gas phase [16,17].

Intermediate temperatures are explored with molecular dynamics simulations. Coarse-grained simulations have indicated patterns on the surface of monolayers, bilayers, etc. [18–20]. In this model, the competition between the electrostatics and the short range interactions are both essential components. We consider a neutral and nonselective homogenous background and choose to model only the charged components. In this manner, large regions of coexistence can be explored, exactly incorporating the electrostatics. The van der Waals interactions are described by a classic 6–12 Lennard-Jones potential

$$U_{\text{LJ}} = 4\varepsilon\left[\left(\frac{\sigma}{r}\right)^{12} - \left(\frac{\sigma}{r}\right)^{6} + C\right] r < r_c, \quad (7)$$

where the potential is cut at a radius $r_c = 2.5\sigma$ and unshifted ($C = 0$) for similarly charged molecules, and the potential is shifted ($C = \frac{1}{4}$) and cut at $r_c = 2^{1/6}\sigma$ for oppositely charged molecules, where σ is an effective molecular radius. The depth of the potential well ε entails a net immiscibility of magnitude ε between oppositely charged species.

We use the ESPRESSO simulation package [21,22] to perform NVT simulations, using a Langevin thermostat. This simulation ensemble matches our analytic work, which assumes constant particle density. The model systems are composed, in the symmetric case, of a mix of $N_+ = 1000$ positively charged and $N_- = 1000$ negatively charged units in a simulation box of size D^3, with $D = 66\sigma$. For the asymmetric case, we used $N_+ = 900$ and $N_{3-} = 300$ (multivalent units with a charge of -3). The molecules are confined to a plane perpendicular to the Z axis, with periodic boundary conditions in the X and Y directions. We explore regions of the phase diagram at surface densities of $\rho = (N_+ + N_-)\pi\sigma^2/4D^2 = 0.36$. The potential between charges is a full Coulomb potential $U_C = l_B T q_1 q_2/r$ calculated using the electrostatic layer correction method [23], which is a 2D correction to P_3M Ewald summation [24]. Late-time snapshots are shown in Fig. 2.

To compare the strong segregation theoretical results with the simulation results, we identify the domain width with $L = [\gamma/(l_B\psi^2)]^{1/2} \sim [\varepsilon/(l_B\psi^{3/2})]^{1/2}$. Here we abandon the assumption of a solid phase density fixed by the molecular radius and consider a line tension γ that scales with the particle density, proportional to the charge density, as $\psi^{1/2}$. This assumes a homogenous swelling of the solid phase density but does not account for vacancy adsorption at interfaces [25,26]. The pattern formation is found to be independent on finite size effects; the density of the solid as well as the periodicity of the solid phase are not significantly changed. The transition appears at the same ratios of short range interactions and strength of the electrostatics.

At small values of ε or low Bjerrum lengths (high temperature), positive and negative regions develop on the surface, and, as the temperature decreases, the domains increase in size. The individual molecular components exhibit hcp packing, with density fluctuations dependent on the temperature. For asymmetric charge ratios $z_+/z_- = \frac{1}{3}$, we show in Fig. 2(a) the formation of a hexagonally patterned "island" at $\rho = 0.10$. For larger densities, as in Fig. 2(b), the solid phase occupies a larger fraction of the space but exhibits more clearly the ordering.

As shown in Figs. 2(c) and 2(d), for symmetric charge ratios $z_+/z_- = 1$, the microstructure is lamellar. We observe phase separation between solid patterned and gas phases. At higher values [Fig. 2(d)], the interfaces are much sharper and exhibit smaller interfacial fluctuations. The orientation of the lamella is perpendicular to the interface; the alignment may be due to the minimization of the local electrostatic energy.

Figures 2(e) and 2(f) show the transition from a solid to a solid-gas coexistence phase for symmetric charge ratios but for weaker electrostatic interactions. At low values of the cohesive energy ε, the system shows the lamellar patterning but possesses large voids between the charged domains, effectively reducing the line tension between domains. Upon further increase of ε, the coexistence re-

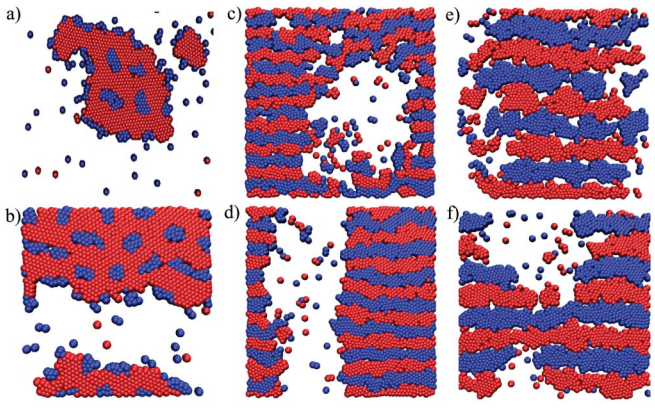

FIG. 2 (color online). Simulation snapshots for systems with charge ratios (a),(b) $z_+/z_- = 1/3$ and (c)–(f) $z_+/z_- = 1$. Frames (a) and (b) illustrate hexagonal order for different densities $\rho_a = 0.10$ and $\rho_b = 0.36$. Frames (c) and (d) show the effect of increased immiscibility $\varepsilon_c = 3.4k_BT$, $\varepsilon_d = 3.7k_BT$, for a fixed Bjerrum length $l_B/\sigma = 0.5$. Frames (e) and (f) show the transition from a homogenous microphase to a phase-segregated state for $\varepsilon_e = 2.6k_BT$, $\varepsilon_f = 2.8k_BT$ for $l_B/\sigma = 0.1$.

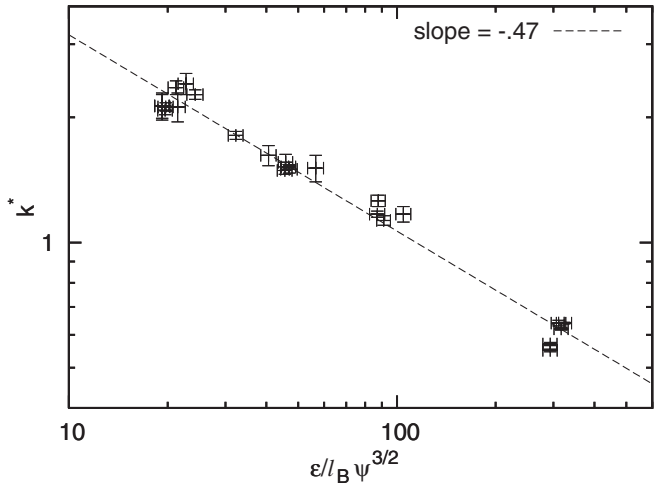

FIG. 3. The location of the peak k^* in the structure factor $S(\vec{k})$ as a function of $\varepsilon/(l_B\psi^{3/2})$, over a range of $l_B/\sigma \sim 0.01$–1. The linear fit shows agreement with the scaling predicted by strong segregation theory of power -0.5.

gion is reached, and the neutral regions segregate to form their own phase, as shown in Fig. 2(f). The lower values of the Bjerrum length in these cases produce larger lamellar sizes, compared with those of Figs. 2(c) and 2(d).

The 2D Fourier transform of the correlation function in the phase-segregated state $\langle \rho_k \rho_{-k} \rangle$ displays a peak at values k^* corresponding to the inverse lamellar spacing in the direction perpendicular to the lamellas. The peak should scale as $k^* \sim [\varepsilon/(l_B\psi^{3/2})]^{-1/2}$. In our simulations, over a range of $l_B/\sigma \sim 0.01$–1, the peak scaling fits through a line of slope -0.47 ± 0.02 when plotted against the group $\varepsilon/(l_B\psi^{3/2})$, as shown in Fig. 3.

By use of analytic techniques, a combination of RPA and strong segregation theory, in addition to molecular dynamics simulations, we demonstrate the possibility of coexistence of periodic ionic domains with a low charge density homogenous phase. Simulations show that, with a simple rescaling of the line tension γ, with charge density $\psi^{1/2}$, low temperature results can be extrapolated to intermediate temperature regimes. The competition between electrostatic and van der Waals interactions at the interface provides a guideline to generate well-controlled, self-assembled surface patterns. Phase segregation phenomena on surfaces and interfaces exhibit rich behavior. Ionic domains may be crucial to increase reaction rates among adsorbed biomolecules at liquid interfaces, a useful tool in biotechnology [27,28].

This work was supported by NSF Grants No. DMR-0414446, No. DMR-0520513, and No. EE-0503943. We acknowledge helpful discussions with Y. Velichko and G. Vernizzi. S. M. L. thanks the hospitality of Christian Holm group, including Axel Arnold and Bernward Mann, where this work was initiated.

[1] S. L. Veatch and S. L. Keller, Phys. Rev. Lett. **89**, 268101 (2002).
[2] D. Zhang, M. A. Carignano, and I. Szleifer, Phys. Rev. Lett. **96**, 028701 (2006).
[3] F. J. Solis, S. I. Stupp, and M. Olvera de la Cruz, J. Chem. Phys. **122**, 054905 (2005).
[4] L. Ramos, T. C. Lubensky, N. Dan, P. Nelson, and D. A. Weitz, Science **286**, 2325 (1999).
[5] J. A. Zasadzinski, E. Kisak, and C. Evans, Curr. Opin. Colloid Interface Sci. **6**, 85 (2001).
[6] M. Seul and D. Andelman, Science **267**, 476 (1995).
[7] H. M. McConnell, Proc. Natl. Acad. Sci. U.S.A. **86**, 3452 (1989).
[8] D. Andelman, F. Brochard, and J. Joanny, J. Chem. Phys. **86**, 3673 (1987).
[9] T. Garel and S. Doniach, Phys. Rev. B **26**, 325 (1982).
[10] S. C. Glotzer, E. A. Di Marzio, and M. Muthukumar, Phys. Rev. Lett. **74**, 2034 (1995).
[11] R. Jamei, S. Kivelson, and B. Spivak, Phys. Rev. Lett. **94**, 056805 (2005).
[12] T. Yamaue, T. Taniguchi, and M. Doi, Prog. Theor. Phys. Suppl. **138**, 416 (2000), and references therein.
[13] P. Gonzalez-Mozuelos and M. Olvera de la Cruz, J. Chem. Phys. **100**, 507 (1994).
[14] S. M. Loverde, Y. S. Velichko, and M. Olvera de la Cruz, J. Chem. Phys. **124**, 144702 (2006).
[15] V. Y. Borue and I. Y. Erukhimovich, Macromolecules **21**, 3240 (1988).
[16] A. V. Ermoshkin and M. Olvera de la Cruz, Macromolecules **36**, 7824 (2003).
[17] P. Gonzalez-Mozuelos and M. Olvera de la Cruz, J. Chem. Phys. **118**, 4684 (2003).
[18] L. Saiz and M. L. Klein, J. Chem. Phys. **116**, 3052 (2002).
[19] Q. Shi and G. A. Voth, Biophys. J. **89**, 2385 (2005).
[20] S. O. Nielsen, C. F. Lopez, P. B. Moore, J. C. Shelley, and M. L. Klein, J. Phys. Chem. B **107**, 13 911 (2003).
[21] ESPRESSO, http://www.espresso.mpg.de (2002–2005).
[22] H.-J. Limbach, A. Arnold, B. A. Mann, and C. Holm, Comput. Phys. Commun. **174**, 704 (2006).
[23] A. Arnold, J. Joannis, and C. Holm, J. Chem. Phys. **117**, 2496 (2002).
[24] R. W. Hockney and J. W. Eastwood, *Computer Simulation Using Particles* (Hilger, London, 1988).
[25] C. Huang and M. Olvera de la Cruz, Phys. Rev. E **53**, 812 (1996).
[26] C. Huang, P. W. Voorhees, and M. Olvera de la Cruz, Acta Mater. **47**, 4449 (1999).
[27] A. Goldar and J. L. Sikorav, Eur. Phys. J. E **14**, 211 (2004).
[28] J. Groves, Sci. STKE 301 (**2005**) pe45.